Journal of Medicinal Chemistry

ACS AuthorChoice

Article

pubs.acs.org/jmc

Terms of Use

Design, Synthesis, Mechanisms of Action, and Toxicity of Novel 20(*S*)-Sulfonylamidine Derivatives of Camptothecin as Potent Antitumor Agents

Mei-Juan Wang,[†] Ying-Qian Liu,*[,†] Ling-Chu Chang,[‡,§] Chih-Ya Wang,[⊥] Yong-Long Zhao,[†] Xiao-Bo Zhao,[†] Keduo Qian,[⊥] Xiang Nan,[†] Liu Yang,[∥] Xiao-Ming Yang,[⊥] Hsin-Yi Hung,[‡,§] Jai-Sing Yang,[⊗] Daih-Huang Kuo,[#] Masuo Goto,[⊥] Susan L. Morris-Natschke,[⊥] Shiow-Lin Pan,[▽] Che-Ming Teng,[○] Sheng-Chu Kuo,[§] Tian-Shung Wu,[◆] Yang-Chang Wu,[§] and Kuo-Hsiung Lee*[,§,⊥]

[†]School of Pharmacy, Lanzhou University, Lanzhou 730000, PR China

[‡]Graduate Institute of Pharmaceutical Chemistry, China Medical University, Taichung 40402, Taiwan

[§]Chinese Medicine Research and Development Center, China Medical University and Hospital, Taichung, Taiwan

[⊥]Natural Products Research Laboratories, UNC Eshelman School of Pharmacy, University of North Carolina, Chapel Hill, North Carolina 27599, United States

[∥]Environmental and Municipal Engineering School, Lanzhou Jiaotong University, Lanzhou 730000, PR China

[⊗]Department of Pharmacology, China Medical University, Taichung 404, Taiwan

[#]Department of Pharmacy and Graduate Institute of Pharmaceutical Technology, Tajen University, Pingtung 907, Taiwan

[▽]Ph.D. Program for Cancer Biology and Drug Discovery, College of Medical Science and Technology, Taipei Medical University, Taipei 11031, Taiwan

[○]Pharmacological Institute, College of Medicine, National Taiwan University, Taipei 10051, Taiwan

[◆]Department of Chemistry, National Cheng-Kung University, Tainan 701, Taiwan

Supporting Information

ABSTRACT: Twelve novel 20-sulfonylamidine derivatives (**9a**–**9l**) of camptothecin (**1**) were synthesized via a Cu-catalyzed three-component reaction. They showed similar or superior cytotoxicity compared with that of irinotecan (**3**) against A-549, DU-145, KB, and multidrug-resistant (MDR) KBvin tumor cell lines. Compound **9a** demonstrated better cytotoxicity against MDR cells compared with that of **1** and **3**. Mechanistically, **9a** induced significant DNA damage by selectively inhibiting Topoisomerase (Topo) I and activating the ATM/Chk related DNA damage-response pathway. In xenograft models, **9a** demonstrated significant activity without overt adverse effects at 5 and 10 mg/kg, comparable to **3** at 100 mg/kg. Notably, **9a** at 300 mg/kg (i.p.) showed no overt toxicity in contrast to **1** (LD_{50} 56.2 mg/kg, i.p.) and **3** (LD_{50} 177.5 mg/kg, i.p.). Intact **9a** inhibited Topo I activity in a cell-free assay in a manner similar to that of **1**, confirming that **9a** is a new class of Topo I inhibitor. 20-Sulfonylamidine **1**-derivative **9a** merits development as an anticancer clinical trial candidate.

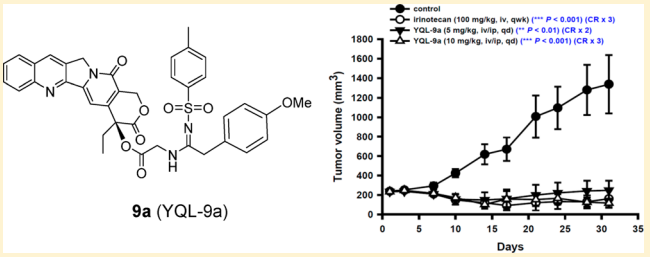

INTRODUCTION

Camptothecin (CPT, **1**, Figure 1) is a naturally occurring alkaloid with remarkable antitumor effects.[1−3] Its antitumor activity has been ascribed to its ability to interfere with the catalytic cycle of DNA topoisomerase I (Topo I) by stabilizing an irreversible drug−enzyme−DNA ternary complex and preventing the religation of single-strand DNA breaks induced by Topo I.[4,5] Intensive synthetic medicinal chemistry efforts over the past decades have led to potent **1**-derivatives, including topotecan (**2**) and irinotecan (**3**), which are now used clinically to treat ovarian, small cell lung, and colon cancers. Also, several derivatives, such as gimatecan (**4**), CKD-602 (**5**), and BNP-1350 (**6**), are in various stages of preclinical or clinical development.[6−8] Although clinically used **1**-derivatives remain a promising class of antitumor agents, their therapeutic use has been severely hindered by toxicity issues and delivery problems, due to poor water solubility, as well as instability of the active lactone form, due to preferential binding of the opened carboxylate to serum albumin.[9,10]

Several approaches, including the development of prodrugs (conjugates and polymer bound camptothecins), new for-

Received: March 6, 2014
Published: July 8, 2014

 © 2014 American Chemical Society

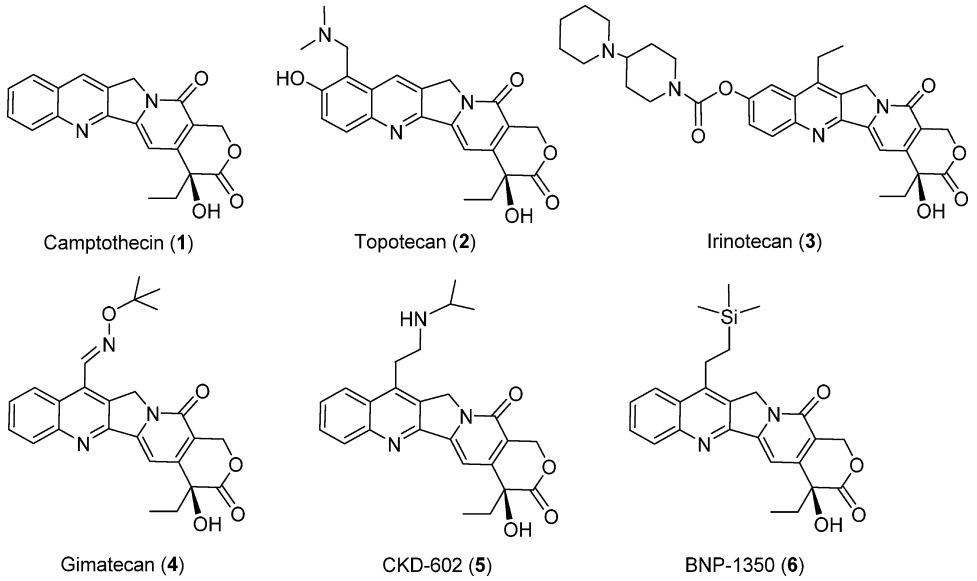

Figure 1. Structures of camptothecin (**1**), topotecan (**2**), irinotecan (**3**), gimatecan (**4**), CKD-602 (**5**), and BNP-1350 (**6**).

Scheme 1. Synthesis of Target Compounds 9a–9l[a]

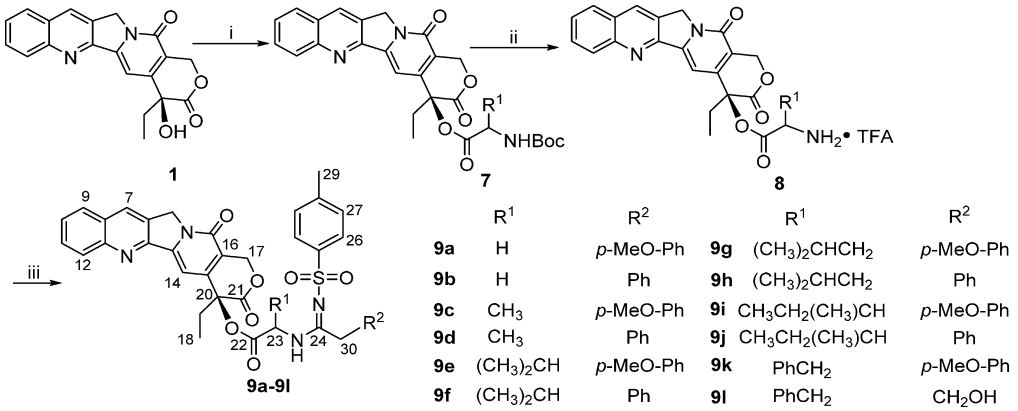

	R^1	R^2		R^1	R^2
9a	H	*p*-MeO-Ph	**9g**	$(CH_3)_2CHCH_2$	*p*-MeO-Ph
9b	H	Ph	**9h**	$(CH_3)_2CHCH_2$	Ph
9c	CH_3	*p*-MeO-Ph	**9i**	$CH_3CH_2(CH_3)CH$	*p*-MeO-Ph
9d	CH_3	Ph	**9j**	$CH_3CH_2(CH_3)CH$	Ph
9e	$(CH_3)_2CH$	*p*-MeO-Ph	**9k**	$PhCH_2$	*p*-MeO-Ph
9f	$(CH_3)_2CH$	Ph	**9l**	$PhCH_2$	CH_2OH

[a]Reagents and conditions: (i) DIPC/DMAP; (ii) 50% TFA-CH_2Cl_2; (iii) alkynes/CuI/TsN_3/Et_3N.

mulations (liposomes or microparticulate carriers), and synthetic lipophilic camptothecins have been explored to improve the antitumor efficiency of the **1**-family.[11−13] Most of these strategies aim to maintain the active closed-lactone form in the plasma compartment. A free 20-hydroxyl group favors lactone ring-opening due to the formation of intramolecular hydrogen bonding,[14] while acylation of this group should stabilize the closed-lactone moiety.[15] Moreover, steric bulk in the introduced ester moiety can be desirable to impede hydrolysis of the ester bond by various enzymes, including carboxylesterases, thereby reducing the toxicity. Indeed, our own results,[16,17] as well as those of others with 20(*S*)-*O*-acyl esters,[18,19] 20(*S*)-*O*-carbonate linked tripeptide conjugates,[20] and 20(*S*)-*O*-linked glycoconjugates,[21] have supported the importance of esterified **1**-derivatives for potent activity. Esterification of the 20-hydroxyl group also enhances plasma stability and augments in vivo antitumor activity compared with those of unmodified **1**.

Amidines are well known as important pharmacophores[22−25] and widely used in bioactive chemicals and drug molecular design. Also, the introduction of a sulfonyl group into a bioactive functional fragment results in significant changes in the compound's bioactivity;[26,27] thus, sulfonylamidines may be useful structural motifs for the optimization of bioactive molecules. Because this group is also quite bulky, it is likely to sterically prevent large enzymes from easily hydrolyzing a 20(*S*)-*O*-acyl ester of **1**, which should also reduce the toxicity. In contrast, SN-38, the compound formed from the hydrolysis of **3**, is quite toxic.[28] Given these considerations, we postulated that the introduction of a sulfonylamidine group at the 20-position of **1** could lead to improved efficacy and reduced toxicity as well as optimize the physicochemical properties of a new **1**-related anticancer drug candidate. Therefore, in the present study, we incorporated the functional fragment sulfonylamidine into **1** at the C-20 position via a Cu-catalyzed one pot reaction[29] and synthesized a novel series of derivatives of **1** as potential antitumor agents.

RESULTS AND DISCUSSION

Chemistry. As shown in Scheme 1, the 20-hydroxyl group of **1** was esterified to furnish *N*-Boc-amino acid derivatives (**7**) in suitable yields by a simple modification of the carbodiimide method using a combination of *N*,*N*′-diisopropyl carbodiimide (DIPC) and 4-dimethylaminopyridine (DMAP). The *N*-Boc group of **7** was removed with trifluoroacetic acid (TFA) in

dx.doi.org/10.1021/jm5003588 | J. Med. Chem. 2014, 57, 6008−6018

Table 1. In Vitro Cytotoxicity Data for 9a–l against Four Human Tumor Cell Lines[a]

	IC_{50} (μM)			
cmpd	A-549	DU-145	KB	KBvin
9a	0.031 ± 0.0035	0.050 ± 0.0038	0.14 ± 0.018	0.026 ± 0.013
9b	0.057 ± 0.0039	0.13 ± 0.011	0.18 ± 0.0008	0.10 ± 0.0073
9c	0.089 ± 0.0083	0.14 ± 0.0059	0.91 ± 0.060	0.087 ± 0.0087
9d	0.071 ± 0.0069	0.15 ± 0.022	0.22 ± 0.017	0.096 ± 0.0094
9e	1.0 ± 0.11	1.7 ± 0.14	11 ± 0.48	1.5 ± 0.11
9f	1.3 ± 0.12	2.0 ± 0.25	11 ± 0.28	2.2 ± 0.056
9g	0.95 ± 0.018	1.6 ± 0.096	2.7 ± 0.0083	1.0 ± 0.13
9h	0.89 ± 0.039	1.1 ± 0.016	4.4 ± 0.42	1.8 ± 0.030
9i	1.2 ± 0.066	8.3 ± 0.14	9.6 ± 0.042	1.7 ± 0.16
9j	6.5 ± 0.43	11 ± 0.75	11 ± 1.0	8.2 ± 0.61
9k	0.12 ± 0.010	0.22 ± 0.025	0.85 ± 0.024	0.12 ± 0.0019
9l	0.083 ± 0.010	0.20 ± 0.013	0.31 ± 0.021	0.14 ± 0.0081
1	0.016 ± 0.0005	0.029 ± 0.0025	0.037 ± 0.0031	0.12 ± 0.0091
3	9.5 ± 0.11	9.3 ± 0.61	9.8 ± 0.48	>20

[a]Each assay was performed in triplicate with duplicated samples, and averaged IC_{50} (μM) values are expressed with standard deviation (SD). A549, lung carcinoma; DU-145, hormone-insensitive prostate cancer; KB, originally isolated from epidermoid carcinoma of the nasopharynx; and KBvin, vincristine-resistant KB subline.

CH_2Cl_2 (1:1) to form the key intermediate TFA salts **8**. Subsequently, we applied a highly efficient Cu-catalyzed three-component coupling reaction,[29] in which **8** was reacted with *p*-toluenesulfonyl azide and a wide range of alkynes to afford the desired compounds **9a–l** in 35–58% yields. The structures of the target molecules were characterized from ^{1}H NMR, ^{13}C NMR, IR, and HR-MS data.

Antiproliferative Activity of New Compounds and Structure–Activity Relationship. The 12 novel **1**-derivatives **9a–l** were evaluated for in vitro antiproliferative activity against four human tumor cell lines, KB (nasopharyngeal), A-549 (lung), DU-145 (prostate), and KBvin (MDR KB subline), by using a sulforhodamine B colorimetric assay with triplicate experiments.[30] Compounds **1** and **3** were used as controls. The screening results are shown in Table 1.

All 12 new compounds (**9a–l**) exhibited significant in vitro cytotoxic activity against the four tested tumor cell lines, with IC_{50} values ranging from 0.026 to 11 μM, indicating that both the R^1 and R^2 groups in the 20-sulfonylamidine side chain might influence the cytotoxic activity of the new **1**-derivatives. The new compounds **9a–l** (except **9a** against KBvin) were less potent than **1**; however, all of the new derivatives showed equivalent or superior cytotoxic activity compared with that of **3**. Among the newly synthesized derivatives, **9a** was the most potent compound against the four tested tumor cell lines. Interestingly, **9a** also showed greater cytotoxic activity against KBvin (IC_{50} 0.026 μM) compared with that of **1** and **3** (IC_{50} 0.12 and >20 μM, respectively). The results also revealed that the A-549 cell line was more sensitive than the other three cell lines to these compounds, which is consistent with the clinical behavior of other **1**-derivatives.[19]

Structure–activity relationship (SAR) correlations were also identified for these new 20-sulfonylamidine derivatives of **1**. When the R^2 group was fixed as phenyl and the R^1 group in the sulfonylamidines was varied, hydrogen (**9b**) and methyl (**9d**) gave the best results compared with those of larger alkyl groups in **9f** (isopropyl), **9h** (isobutyl), and **9j** (*sec*-butyl). Similar results were seen in the corresponding derivatives bearing a *p*-methoxyphenyl R^2 group. For example, against the A-549 cell line, the rank order of cytotoxic potency was **9a** (H) > **9c** (methyl) > **9g** (isobutyl) ≥ **9e** (isopropyl) ≥ **9i** (*sec*-butyl). Therefore, small aliphatic chains appear to be the best R^1 substituents for greater cytotoxic potency. When the R^1 group was kept constant, and the R^2 group was changed from phenyl to *p*-methoxyphenyl, the cytotoxic activity often improved (for example, compare **9b** to **9a**, **9f** to **9e**, **9h** to **9g**, or **9j** to **9i** against KBvin). In addition, compound **9l** bearing a hydroxymethyl R^2 group displayed comparable (DU-145, KB) or greater (A-549, KBvin) cytotoxic activity compared to that of **9k** with a *p*-methoxyphenyl R^2 group. Compound **9k**, which also has a benzyl R^1 group, generally exhibited intermediate potency between compounds with smaller (**9a** and **9c**) and larger (**9e**, **9g**, and **9i**) alkyl R^1 groups. These findings indicated that the cytotoxic profile of **1**-derivatives may be sensitive to the size and electronic density of the substituents at C-20. On the basis of these in vitro results, compound **9a** was selected for in vivo evaluation.

Mechanism of Action Studies on 9a. *Inhibition of Topo I Activity by **9a** in a Cell-Free System.* A **1**-derivative with an esterified 20-hydroxy group is expected to be activated by digestion with carboxylesterases. To determine whether intact **9a** inhibits Topo I, a cell-free Topo I activity assay was employed using purified recombinant human Topo I (Figure 2A). In this assay, supercoiled plasmid DNA is relaxed and nicked by recombinant Topo I. Thus, with the vehicle control or a test compound that has no inhibitory effect on Topo I activity, relaxed and nicked DNA are found. As seen in Figure 2A, **3**, known to be a prodrug of **1**, showed the same result since it cannot be activated in this cell-free system as it is by carboxylesterases in the cell. In contrast, SN-38, a bioactive metabolite of **3**, inhibited Topo I activity. Notably, we found that intact **9a** inhibited Topo I activity in this cell-free assay in a manner similar to that of **1** (Figure 2A). We authenticated the inhibitory effect of **9a** against Topo I in a dose-dependent manner (Figure 2B). Thus, we confirmed that **9a** is a new class of Topo I inhibitor.

*Induction of Apoptosis by **9a** in Human Tumor Cells.* Because A-549 human lung adenocarcinoma epithelial cells displayed higher sensitivity than the other tested cancer cell lines to **9a** in the preliminary cytotoxicity profile, A-549 cells were used in our mechanistic study. Initially, we investigated morphological cellular changes. After exposure to **9a**, A-549

dx.doi.org/10.1021/jm5003588 | J. Med. Chem. 2014, 57, 6008–6018

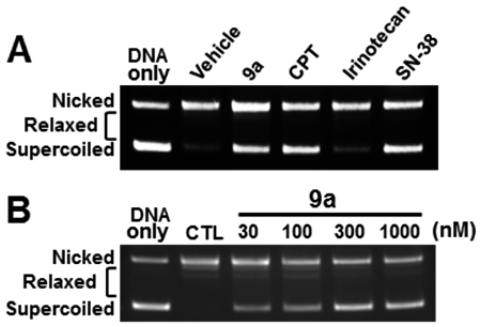

Figure 2. Compound **9a** directly inhibits Topo I in a cell-free system. (A) Recombinant human Topo I was incubated with the vehicle (CTL), 100 nM **9a**, 100 nM **1** (CPT), or 1 μM **3** (Irinotecan) followed by incubation with supercoiled plasmid DNA. Plasmid DNA was separated by agarose gel and stained with ethidium bromide. SN-38 (100 nM), an active metabolite of **3**, was used as a positive control. (B) Dose-dependent inhibition of Topo I by **9a**. Recombinant human Topo I was incubated with supercoiled plasmid DNA in the presence of different concentrations of **9a** as indicated. These results show that **9a** directly inhibits recombinant human Topo I in a dose–response manner.

cells showed apoptotic morphological features, including cell shrinkage and membrane blebbing (Figure 3A). Apoptosis induction was further confirmed by double staining with FITC-annexin V and propidium iodide, showing that **9a** treatment increased the percentage of apoptotic cells (annexin V positive cell population: vehicle versus **9a**, 24 h, 1.1% versus 3.7%, $P < 0.01$; 48 h, 2.0% versus 34.1%, $P < 0.001$) (Figure 3B). Western blot analysis showed that cleaved caspases, the executors of apoptosis, were formed in response to **9a**, including caspase-8, -9, and -3 (Figure 3C). PARP, a hallmark of apoptosis, was also activated by **9a** (Figure 3C). These data demonstrated that **9a** inhibits A-549 cell growth through apoptosis induction.

*Activation of DNA Damage Response Pathway by **9a**.* The main effect of **1** is to bind to and stabilize the covalent Topo I-DNA complex, thus the induction of cell cycle delay in S phase, preventing DNA ligation and eventually leading to apoptosis.[31] Whether **9a** activates the same pathway as **1** in A-549 cells was examined to demonstrate the mechanism of action. First, we determined the effect of **9a** on cell cycle distribution using flow cytometry analysis (Figure 4A). As we expected, treatment with **9a** for 24 h resulted in increased cell populations in S and sub-G_1 phases. A Topo I-mediated DNA cleavage assay was performed to examine whether **9a** exhibits an inhibitory effect on Topo I activity in the cell. The results showed that **9a** inhibited the relaxation of supercoiled DNA, which is similar to the effect of **1** (Figure 4B). However, both **9a** and **1** failed to decatenate kineoplast DNA (kDNA), whereas etoposide, a known Topo II inhibitor, effectively blocked the decatenation of kDNA (Figure 4C). Because it has been shown that **1**-Topo I-DNA covalent complexes enhance the transcription-dependent degradation of Topo I via a 26S proteasome pathway,[32] the effects of **9a** on the expression levels of Topo I and Topo II were investigated. Western blot analysis showed that **9a** significantly inhibited protein levels of Topo I after 8 h of treatment and slightly affected levels of Topo IIα and Topo IIβ after 24 h treatment (Figure 4D). These results

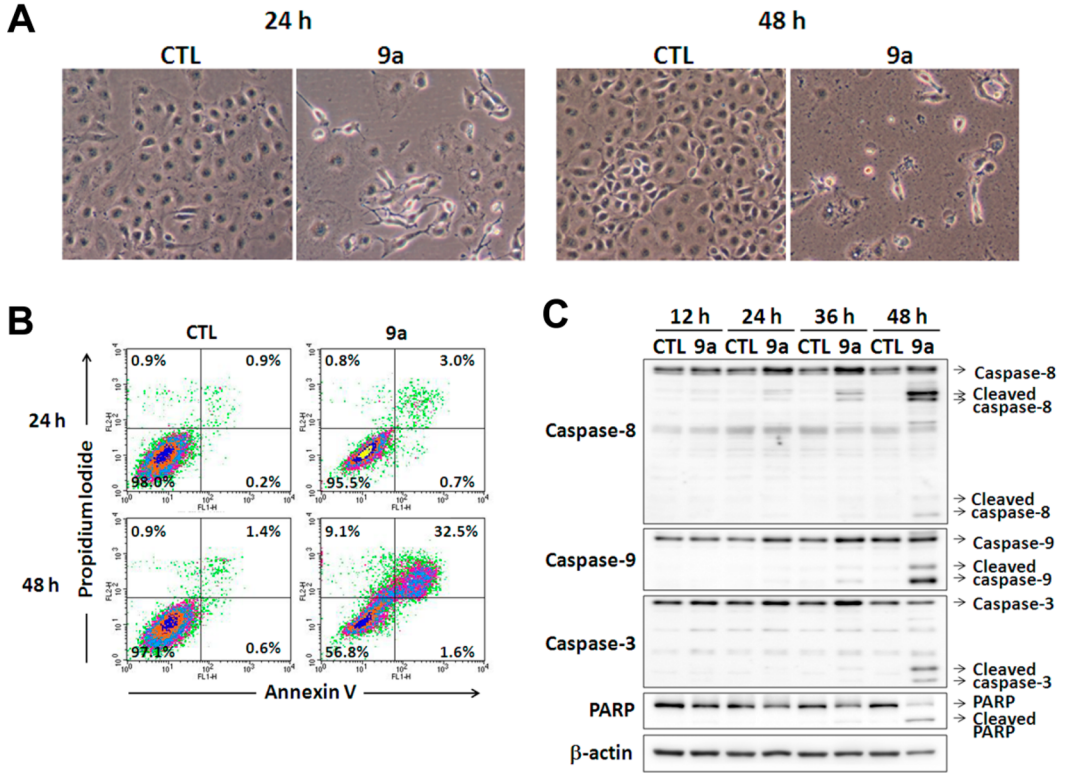

Figure 3. Induction of apoptosis by **9a**. (A) Compound **9a** induced apoptotic morphological alternation. A-549 cells were incubated in the absence or presence of 100 nM **9a** for 24 or 48 h. Morphological changes were observed under a phase-contrast microscope. (B) Compound **9a** induces apoptosis. A-549 cells were treated with the vehicle (CTL) or 100 nM **9a** for 24 or 48 h followed by FITC-annexin V with propidium iodide double staining. Percentages of apoptotic cells were analyzed by flow cytometry. (C) Compound **9a** activates caspases. A-549 cells were treated with 100 nM **9a** at indicated times. Cells were harvested and lysed for the determination of caspase cleavage using Western blot analysis.

dx.doi.org/10.1021/jm5003588 | J. Med. Chem. 2014, 57, 6008–6018

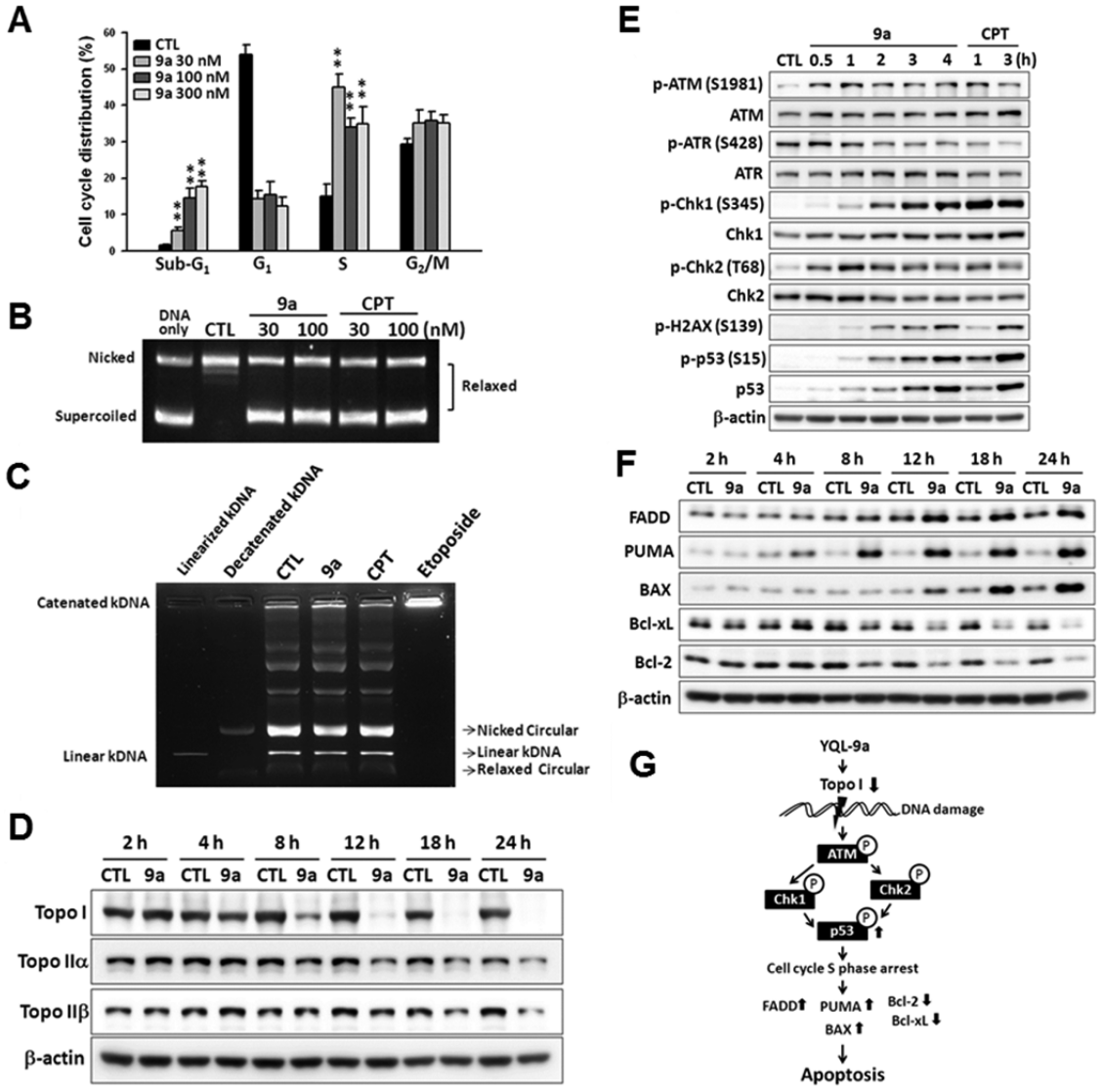

Figure 4. Mechanisms of action of **9a**. (A) Accumulation of S phase by **9a**. Cell cycle distribution of A-549 was analyzed by a flow cytometer after treatment with 0 (CTL), 30, 100, or 300 nM **9a** for 24 h followed by staining with propidium iodide. **, $P < 0.01$. (B) Inhibition of Topo I activity by **9a** in vitro. A-549 cells were treated with the vehicle (CTL), **9a** (30, 100 nM), or **1** (30, 100 nM) for 1 h. Cells were harvested for Topo I activity assay as described in Experimental Section. (C) Selective inhibition of Topo I by **9a**. A-549 cells were treated with **9a** (100 nM), **1** (100 nM), or Topo II inhibitor etoposide (30 μM) for 1 h, followed by the Topo II activity assay. (D) Depression of Topo I expression by **9a**. A-549 cells were treated with vehicle (CTL) or 100 nM **9a** for the indicated hours. Whole cell lysates were analyzed by Western blotting using antibodies to Topo I, Topo IIα, Topo IIβ, and β-actin as a loading control. These results demonstrated that compound **9a** selectively inhibited Topo I activity and expression. (E) Activation of DNA damage checkpoint proteins by **9a**. Whole cell extracts were prepared from A-549 cells treated with 100 nM **9a** or 100 nM **1** for the indicated hours. Phosphorylation of DNA damage checkpoint proteins were detected by Western blotting using specific antibodies to phosphorylated ATM (p-ATM), ATR (p-ATR), Chk1 (p-Chk1), Chk2 (p-Chk2), p-H2AX, and p53 (p-p53) as indicated. Total amount of each protein and β-actin was detected by the pan antibody to each protein as the loading control. (F) Activation of apoptosis pathway by **9a**. Whole cell lysates were prepared from A-549 cells treated with 100 nM **9a** or vehicle (CTL) for the indicated hours followed by detection of apoptosis-related proteins as indicated. (G) Schematic representation of the mechanisms of action of **9a**. Compound **9a** (YQL-9a) directly inhibits Topo I enzymatic activity and depresses Topo I expression, which results in DNA damage checkpoint activation, cell cycle delay at S phase, and subsequently apoptosis pathway stimulation.

clearly demonstrated that **9a** inhibited Topo I without interfering with Topo II activity. Compound **9a** acts directly on Topo I and results in the accumulation of covalent Topo I-DNA complexes followed by proteasomal Topo I degradation, which is the same effect as **1**, and contributes to **9a**'s cytotoxicity.

Compound **1** can induce DNA damage and activate the ATM-Chk2 DNA damage-response pathway to trigger apoptotic pathways in cancer cells.[33] We found that ATM underwent phosphorylation at the Ser1981 residue after 0.5 h treatment with **9a** (Figure 4E). Activation of ATM kinase was confirmed by detecting the phosphorylation of downstream effectors, Chk1, Chk2, and histone H2AX (Figure 4E). Phosphorylation of H2AX at the Ser139 residue (γH2AX) indicated that **9a** caused DNA double-strand breaks. P53 plays a critical role in DNA-damage functions, including cell cycle regulation and apoptosis triggering.[34] The up-regulation and phosphorylation of p53 were greatly enhanced by **9a** (Figure 4E). P53 downstream apoptotic proteins such as PUMA and BAX were also predominantly increased by **9a**. Furthermore, **9a**

dx.doi.org/10.1021/jm5003588 | J. Med. Chem. 2014, 57, 6008−6018

up-regulated FADD, a component of death receptor-mediated extrinsic apoptosis, and down-regulated the pro-survival proteins Bcl-xL and Bcl-2 by preventing leakage of mitochondrial damage contents (Figure 4F).

Taken together, compound **9a** (YQL-9a) directly inhibits Topo I activity and depresses Topo I expression, which induces cell cycle delay at S phase as well as activation of the DNA damage-response pathway, and subsequently activates the apoptosis pathway (Figure 4G). Our data support the superiority of **9a** over parent compound **1**, suggesting that **9a** is an excellent potential anticancer drug candidate. Therefore, we further investigated the antitumor activity of **9a** and toxicological evaluation in vivo.

*Antitumor Activity of **9a** in Vivo.* Xenograft model antitumor assay using human colorectal adenocarcinoma cell line HCT116 was performed according to the regimen in Table 2. The 31-day study utilized four groups of mice (n = 8) bearing established HCT116 xenograft with mean volumes of approximately 200 mm^3 on day one. The tumor growth and animal body weight change for each treatment group were measured three times per week (Figure 5). Compound **9a** was administered intravenously (i.v.) for 7 days and then intraperitoneally (i.p.) at 5 and 10 mg/kg once every day (QD) to the end. Two of eight and three of eight mice showed complete regression in the 5 mg/kg and 10 mg/kg dose groups, respectively. There were no significant changes in body weight at either dose. The experimental control using **3** also exhibited antitumor activity at a dose of 100 mg/kg once every week (QWK) (P < 0.001), and three mice showed complete regression, supporting the accuracy of our in vivo evaluation. On the basis of the Student's t-test evaluation, **9a** at 5 mg/kg (P < 0.01) and 10 mg/kg (P < 0.001) exhibited significant antitumor activity in vivo without overt signs of symptoms and an anaphylactic reaction.

Table 2. Study Design of the Xenograft Model Antitumor Assay[a]

		treatment regimen		
group	n	agent	mg/kg	schedule
1	8	vehicle		QD
2	8	**9a**	5	QD
3	8	**9a**	10	QD
4	8	**3**	100	QWK

[a]Saline containing 5% DMSO and 5% cremophor were used as the vehicle. QD, once every day. QWK, once every week.

*Toxicological Evaluation of **9a** in Mice.* Acute toxicity of **9a** in the mouse was evaluated pathologically. Sixty 8-week-old male BALB/c mice were randomized into six groups (n = 10) to receive 0 (vehicle only), 30, 100, 200, or 300 mg/kg of **9a** i.p. on day zero. One group was kept without treatment as a normal control. All treated animals showed no anaphylactic responses, allergic reactions, or significant body weight loss (Figure 6A) and were as healthy as the normal control animals, indicating significantly reduced toxicity compared with that of **1** (LD_{50} = 56.2 mg/kg, i.p.) and **3** (LD_{50} = 177.5 mg/kg, i.p.).[35] At the end of the experimental period, all animals were euthanized, and tissues from the liver, lung, kidney, and spleen were evaluated histopathologically according to the guidelines described by Shackelford et al.[36] as well as being graded for symptomatic lesions. Histopathological evaluations included (1) glycogen deposition, inflammatory cell infiltration, and focal necrosis in the liver (Figure 6B), (2) regeneration of renal tubule, inflammatory cell infiltration, and chronic progressive nephropathy in kidney, and (3) inflammatory cell infiltration and adenoma in the lung (Figure 6C). Although a few microscopic lesions were observed in tissues from both **9a**-treated and untreated mice, all lesions were considered spontaneous lesions and were not related to the administration of **9a**. Thus, **9a**-treated animals showed no adverse effects according to hepatic, splenic, kidney, and lung parameters. Thus, the animals apparently tolerated treatment with 300 mg/kg of **9a**, portending an acceptable safety profile.

We postulate that the toxicological improvement against normal tissues might be associated with the introduction of a sulfonylamidine side chain at the 20-position of **1**. Surprisingly, this modification does not disrupt the inhibitory effect against Topo I and may also prevent lactone ring-opening resulting in stabilization of the closed lactone moiety and contributing to

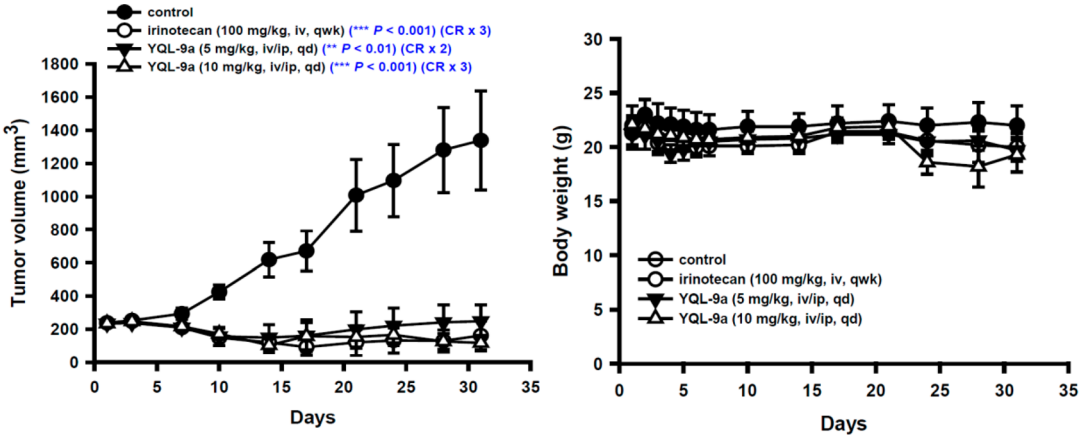

Figure 5. Potent antitumor activity of **9a** in vivo. A xenograft model antitumor assay was performed using human colorectal HCT116 cells. When the tumor graft volume reached about 200 mm^3, mice were randomly separated into four groups (n = 8), and administration of compound was started according to the treatment regimen as shown in Table 2 (left panel). Compound **9a** (YQL-9a) potently prevented tumor growth at 5 or 10 mg/kg compared with the vehicle (control), without significant effect on body weight (right panel). Furthermore, two or three mice administered **9a** at 5 or 10 mg/kg, respectively, underwent complete regression (CR). Compound **3** (irinotecan) was used as an experimental control, and three mice displayed CR. These results were statistically significant (P < 0.01, Student's t-test).

dx.doi.org/10.1021/jm5003588 | J. Med. Chem. 2014, 57, 6008−6018

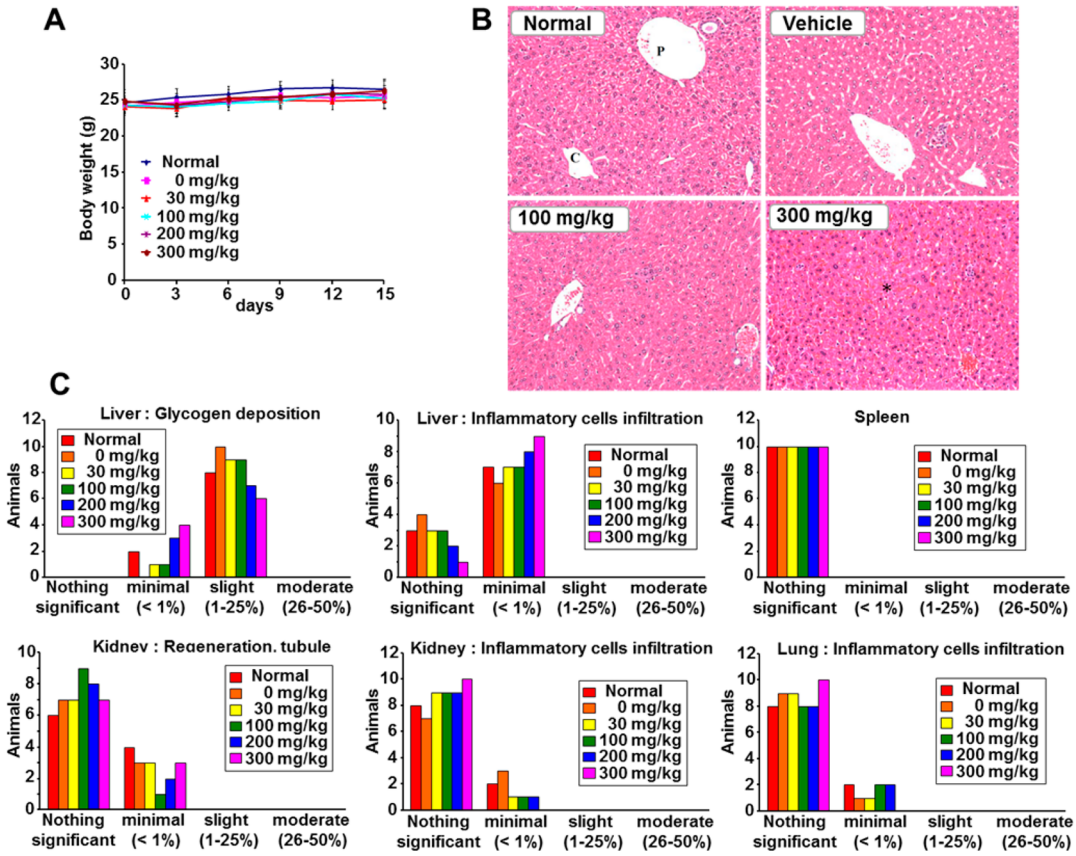

Figure 6. Pathological evaluation of toxicity of **9a** in mice. (A) No significant effect on body weight. Sixty BALB/c mice were randomly divided into six groups, and 10 animals in each group received an i.p. injection of **9a** at 0 (vehicle), 30, 100, 200, or 300 mg/kg, or did not receive an injection at all (normal). (B) Histopathological examination of hepatotoxicity. Formalin-fixed livers from animals without (normal) or with injection of vehicle, 100 mg/kg **9a** or 300 mg/kg **9a**, were embedded in paraffin. Tissue sections were stained with hematoxyline and eosin (H&E). Stained sections were evaluated histopathologically for glycogen deposition, focal necrosis, and inflammatory cell infiltration. Central vein (C) and portal tract (P) were indicated (upper left panel). Post-mortem change was labeled (*). (C) Summary of histopathological evaluation of toxicity. Tissues from the liver, spleen, kidney, and lung were fixed with formalin and embedded in paraffin. Tissue sections were evaluated histopathologically as indicated after staining with H&E. These results demonstrated that the body weight, liver, spleen, kidney, and lung were not affected by treatment with **9a**, even at 300 mg/kg.

better bioactivity of **1**. Further studies including metabolic and pharmacokinetic evaluations, as well as introduction of a sulfonylamidine side chain at the C-7 position of **1**, are currently underway to address this supposition.

CONCLUSIONS

In summary, a novel series of 20(*S*)-sulfonylamidine **1**-derivatives were designed and synthesized with a key step being a Cu-catalyzed one pot reaction. All 12 derivatives showed comparable or superior cytotoxic activity compared with that of **3**. Notably, compound **9a** was as potent as **1** and far more potent than **3** against multidrug-resistant KBvin cells. The IC_{50} values of the new derivatives ranged from 0.026 to 11 μM, indicating that the R^1 and R^2 groups in the 20-sulfonylamidine side chain could greatly influence the cytotoxic activity of the new **1**-derivatives, leading to important SAR information. Also, **9a** at 5 mg/kg and 10 mg/kg demonstrated significant antitumor activity in mice bearing established human HCT116 colorectal adenocarcinoma with no significant changes in body weight at all doses tested. In addition, two of eight and three of eight mice showed complete regression in the 5 mg/kg and 10 mg/kg dose groups, respectively. Histopathological evaluation of acute toxicity against the liver, spleen, lung, and kidney in mice showed no adverse effects of **9a** treatment with 300 mg/kg. On the basis of these positive results, further development of **9a**-related compounds as potential anticancer clinical trial candidates is definitely warranted.

EXPERIMENTAL SECTION

Chemistry General Information. *N*-Boc-amino acids and TFA were purchased from GL Biochem (Shanghai) Company. DIPC and DMAP were purchased from Sigma Chemical Company (China). Other reagents and solvents were purchased from commercial sources and were used as received. The starting compound **1** was isolated from the Chinese medicinal plant *C. acuminata* and was purified before being used (>98% pure). Analytical thin-layer chromatography (TLC) and preparative thin-layer chromatography (PTLC) were performed with silica gel plates using silica gel 60 GF254 (Qingdao Haiyang Chemical Co., Ltd.). Melting points were taken on a Kofler melting point apparatus and are uncorrected. IR spectra were obtained on an NIC-5DX spectrophotometer. MS analyses were performed on ZAB-HS and Bruker Daltonics APEXII49e instruments. NMR spectra were recorded on a Bruker AM-400 spectrometer at 400 MHz using TMS as reference (Bruker Company, USA). The purity of all tested compounds was determined by HPLC (Agilent Technologies 1100 series) equipped with a C-18 bound-phase column (Eclipse Plus C18, 5 μM particle size, 4.6 mm × 250 mm). A gradient elution was performed with MeOH and water as a mobile phase and was monitored at 254 nm. All tested compounds were >95% pure.

dx.doi.org/10.1021/jm5003588 | *J. Med. Chem.* 2014, 57, 6008−6018

Synthesis of Key Intermediates 7 and 8. The appropriate *N*-Boc-amino acid (3.13 mmol) was dissolved in 200 mL of anhydrous CH_2Cl_2 at rt. To this solution, DIPC (0.5 mL, 3.13 mmol), DMAP (3.13 mmol), and **1** (3.13 mmol) were added at 0 °C.[16] The reaction mixture was allowed to warm to rt and left for 16 h. The solution was then washed with 0.1 N HCl, dried, and evaporated under reduced pressure to yield a white solid, which was recrystallized from MeOH to give a *N*-Boc-amino acid **1** ester derivative (**7**) in 56−87% yield. Subsequently, this intermediate (**7**, 1 mmol) was dissolved in a mixture of CH_2Cl_2 (10 mL) and TFA (10 mL) and stirred at rt for 1 h. The solvent was removed, and the remaining solid was recrystallized from CH_2Cl_2 and diethyl ether to give the corresponding TFA salt (**8**) in 57−82% yield.

General Synthetic Procedure for Compounds 9a−91. Triethylamine (1.2 mmol) was added slowly to a suspension of the TFA salt **8** (0.5 mmol) in CH_2Cl_2 (35 mL), and this mixture was stirred for 10 min until a clear solution was obtained. Under an N_2 atmosphere, alkyne (0.5 mmol), *p*-toluenesulfonyl azide (0.6 mmol), and CuI (0.05 mmol) were added. The reaction mixture was stirred for 2−6 h at rt. After the reaction was completed, as monitored by TLC, the reaction mixture was diluted by adding CH_2Cl_2 (4 mL) and aqueous NH_4Cl solution (6 mL). The mixture was stirred for an additional 30 min, and two layers were separated. The aqueous layer was extracted with CH_2Cl_2 (3 mL × 3). The combined organic layers were dried over $MgSO_4$, filtered, and concentrated in vacuo. The crude residue was purified by flash column chromatography on Si gel using $CHCl_3$−MeOH (10:1−20:1) as eluent to give **9a−9l**. HPCL chromatograms and conditions for all 12 new compounds (**9a−9l**) are provided as Supporting Information.

Compound 9a. Yield 52%; mp 129−131 °C; t_R-HPLC, 3.59 min (95.4%). IR (KBr) ν cm^{-1}: 3376, 3285, 2932, 1753, 1663, 1612, 1510, 1455, 1401, 1277, 1249, 1144, 1089, 1053, 892, 789, 688, 553; ^{1}H NMR ($CDCl_3$, 400 MHz) δ 8.39 (s, 1H, C7−H), 8.24 (d, 1H, J = 8.8 Hz, C9−H), 7.94 (d, 1H, J = 8.0 Hz, C12−H), 7.85 (t, 1H, J = 7.6 Hz, C11−H), 7.82 (d, 2H, J = 8.0 Hz, Ts-H), 7.68 (t, 1H, C10−H), 7.32 (s, 1H, C14−H), 7.24 (d, 2H, J = 8.0 Hz, Ts-H), 7.04 (d, 2H, J = 8.4 Hz, -PhOCH$_3$), 6.83 (d, 2H, J = 8.8 Hz, -PhOCH$_3$), 5.52 (ABq, 2H, J = 17.2, C17−H), 5.26 (s, 2H, C5−H), 4.17−4.31 (m, 4H, C23, 30-H), 3.73 (s, 3H, -PhOCH$_3$), 2.39 (s, 3H, Ts-CH$_3$), 2.11−2.21 (m, 2H, C18−H), 0.91 (m, 3H, C19−H); ^{13}C NMR (100 MHz, $CDCl_3$) δ 167.6, 167.1, 166.8, 159.4, 157.1, 152.2, 148.9, 146.7, 144.8, 131.3, 131.2, 130.8, 129.7, 129.2, 128,4, 128.2, 126.5, 142.4, 140.2, 120.1, 114.9, 95.6, 76.7, 67.2, 55.2, 50.0, 43.3, 38.5, 31.8, 21.5, 7.5. HRMS calcd for $C_{38}H_{34}N_4O_8S$: 729.1990 [M + Na]$^+$; found, 729.2002 [M + Na]$^+$.

Compound 9b. Yield 54%; mp132−134 °C; t_R-HPLC, 3.33 min (100%). IR (KBr) ν cm^{-1}: 3394, 3339, 3061, 2973, 2926, 1753, 1663, 1614, 1557, 1498, 1453, 1401, 1278, 1232, 1145, 1089, 1054, 985, 813; ^{1}H NMR ($CDCl_3$, 400 MHz) δ 8.39 (s, 1H, C7−H), 8.24 (d, 1H, J = 8.8 Hz, C9−H), 7.94 (d, 1H, J = 8.0 Hz, C12−H), 7.82−7.86 (m, 3H, C11−H, Ts-H), 7.68 (t, 1H, C10−H),7.33 (s, 1H, C14−H), 7.28−7.32 (m, 3H, Ph-H), 7.23 (d, 2H, J = 8.0 Hz, Ts-H), 7.18 (d, 2H, J = 8.0 Hz, Ph-H), 5.51 (ABq, 2H, J = 17.2 Hz, C17−H), 5.26 (s, 2H, C5−H), 4.20−4.31 (m, 4H, C23, 30-H), 2.39 (s, 3H, Ts-CH$_3$), 2.11−2.22 (m, 2H, C18−H), 0.91 (m, 3H, C19−H); ^{13}C NMR (100 MHz, $CDCl_3$) δ 167.6, 166.8, 166.5, 157.2, 152.2, 148.9, 146.4, 144.8, 132.3, 131.2, 130.8, 130.1, 129.7, 129,5, 128.3, 126.5, 142.4, 140.2, 120.2, 95.6, 76.2, 67.2, 50.0, 43.3, 39.3, 31.7, 21.5, 7.5. HRMS calcd for $C_{37}H_{32}N_4O_7S$: 677.2064 [M + Na]$^+$; found, 677.2051 [M + Na]$^+$.

Compound 9c. Yield 55%; mp 112−114 °C; t_R-HPLC, 2.92 min (96.9%). IR (KBr) ν cm^{-1}: 3371, 3261, 2931, 1751, 1662, 1611, 1548, 1402, 1277, 1249, 1144, 1085, 814, 759, 689; ^{1}H NMR ($CDCl_3$, 400 MHz) δ 8.38 (s, 1H, C7−H), 8.26 (d, 1H, J= 8.8 Hz, C9−H), 7.93 (d, 1H, J = 8.0 Hz, C12−H), 7.80−7.83 (m, 3H, C11−H, Ts-H), 7.67 (t, 1H, C10−H), 7.36 (s, 1H, C14−H), 7.22 (d, 2H, J = 8.0 Hz, Ts-H), 7.02 (d, J = 8.8 Hz, -PhOCH$_3$), 6.81 (d, 2H, J = 8.8 Hz, -PhOCH$_3$), 5.50 (ABq, 2H, J = 17.2 Hz, C17−H), 5.26 (s, 2H, C5−H), 4.86 (m, 1H, C23−H), 4.23 (s, 2H, C30−H), 3.74 (s, 3H, -PhOCH$_3$), 2.39 (s, 3H, Ts-CH$_3$), 2.11−2.21 (m, 2H, C18−H), 1.47 (m, 3H, L-alanine-CH$_3$), 0.91 (m, 3H, C19−H); ^{13}C NMR (100 MHz, $CDCl_3$) δ 170.8, 166.8, 166.3, 159.4, 157.2, 152.1, 148.9, 146.6, 144.7, 131.4, 131.1, 130.7, 130.5, 129.8, 129.5, 129.1, 128.4, 128.2, 128.0, 126.4, 124.3, 142.2, 140.3, 120.8, 114.8, 95.5, 67.2, 55.2, 50.0, 49.7, 38.6, 31.7, 21.5, 17.4, 7.5. HRMS calcd for $C_{39}H_{36}N_4O_8S$: 743.2146 [M + Na]$^+$; found, 743.2157[M + Na]$^+$.

Compound 9d. Yield 57%, 108−110 °C; t_R-HPLC, 3.55 min (100%). IR (KBr) ν cm^{-1}: 3395, 3311, 2979, 1755, 1667, 1619, 1541, 1402, 1277, 1231, 1143, 1085, 1058, 813, 755, 702; ^{1}H NMR ($CDCl_3$, 400 MHz) δ 8.39 (s, 1H, C7−H), 8.22 (d, 1H, J = 8.4 Hz, C9−H), 7.94 (d, 1H, J = 8.0 Hz, C12−H), 7.80−7.89 (m, 3H, C11−H, Ts-H), 7.69 (t, 1H, C10−H), 7.38−7.41 (m, 2H, Ph-H), 7.36 (s, 1H, C14−H), 7.30−7.33 (m, 3H, Ph-H), 7.25 (d, 2H, J = 8.0 Hz, Ts-H), 5.51 (ABq, 2H, J = 17.2 Hz, C17−H), 5.25 (s, 2H, C5−H), 4.82 (m, 1H, C-23H), 4.33 (s, 2H, C30−H), 2.40 (s, 3H, Ts-CH$_3$), 2.11−2.21 (m, 2H, C18−H), 1.44 (d, 3H, L-alanine-CH$_3$), 0.89 (m, 3H, C19−H); ^{13}C NMR (100 MHz, $CDCl_3$) δ 170.0, 166.7, 165.7, 157.2, 152.2, 148.9, 146.7, 144.6, 132.6, 131.1, 130.7, 130.2, 129.8, 129.5, 129.4, 129.2, 128.4, 128.2, 128.1, 126.4, 142.2, 140.2, 120.2, 95.3, 67.2, 50.0, 49.9, 39.5, 31.7, 21.5, 17.3, 7.5. HRMS calcd for $C_{38}H_{34}N_4O_7S$: 691.2221[M + H]$^+$; found, 691.2206 [M + H]$^+$.

Compound 9e. Yield 55%; mp 118−120 °C; t_R-HPLC, 4.40 min (95.2%). IR (KBr) ν cm^{-1}: 3392, 3259, 2931, 1749, 1665, 1615, 1541, 1511, 1401, 1277, 1249, 1142, 1086, 812, 689, 553; ^{1}H NMR ($CDCl_3$, 400 MHz) δ 8.38 (s, 1H, C7−H), 8.20 (d, 1H, J= 8.8 Hz, C9−H), 7.94 (d, 1H, J = 8.0 Hz, C12−H), 7.82 (t, 1H, C11−H), 7.72 (d, 2H, J = 8.4 Hz, Ts-H), 7.66 (t, 1H, C10−H), 7.42 (d, 2H, J = 8.4 Hz, -PhOCH$_3$), 7.36 (s, 1H, C14−H), 7.17 (d, 2H, J = 8.0 Hz, Ts-H), 7.04 (d, 2H, J = 8.8 Hz, -PhOCH$_3$), 5.51 (ABq, 2H, J = 17.6 Hz, C17−H), 5.26 (s, 2H, C5−H), 4.61 (m, 1H, C23−H), 4.33 (s, 2H, C30−H), 3.80 (s, 3H, -PhOCH$_3$), 2.36 (s, 3H, Ts-CH$_3$), 2.18−2.20 (m, 3H, C18−H, L-valine-CH(CH$_3$)$_2$), 0.91 (m, 3H, C19−H), 0.74−0.89 (m, 6H, L-valine-CH(CH$_3$)$_2$); ^{13}C NMR (100 MHz, $CDCl_3$) δ 168.4, 166.9, 166.6, 159.6,157.2, 152.2, 148.9, 146.7, 144.1, 131.7, 131.0, 130.6, 129.8, 129.0, 128.4, 128.3, 128.1, 128.0, 126.2, 142.2, 140.2, 120.8, 115.1, 95.5, 76.3, 67.4, 59.2, 55.3, 50.1, 38.8, 31.7, 31.0, 21.4, 17.7, 7.5. HRMS calcd for $C_{41}H_{40}N_4O_8S$: 749.2640 [M + H]$^+$; found, 749.2648 [M + H]$^+$.

Compound 9f. Yield 53%; mp 112−114 °C; t_R-HPLC, 4.53 min (95.1%). IR (KBr) ν cm^{-1}: 3399, 3263, 2964, 1752, 1666, 1620, 1561, 1534, 1455, 14399, 1277, 1256, 1141, 1085, 992, 806; ^{1}H NMR ($CDCl_3$, 400 MHz) δ 8.38(s, 1H, C7−H), 8.20 (d, 1H, J= 8.8 Hz, C9−H), 7.93 (d, 1H, J = 8.0 Hz, C12−H), 7.80 (t, 1H, C11−H), 7.73 (d, 2H, Ts-H), 7.66 (t, 1H, C10−H), 7.48−7.53 (m, 5H, Ph-H), 7.36 (s, 1H, C14−H), 7.16 (d, 2H, J = 8.0 Hz,Ts-H), 5.51 (ABq, 2H, J = 17.2 Hz, C17−H), 5.26 (s, 2H, C5−H), 4.60 (m, 1H, C23−H), 4.23 (s, 2H, C30−H), 2.35 (s, 3H, Ts-CH$_3$), 2.18−2.20 (m, 3H, C18−H, L-valine-CH(CH$_3$)$_2$), 0.91(m, 3H, C19−H), 0.74−0.89 (m, 6H, L-valine−CH(CH$_3$)$_2$); ^{13}C NMR (100 MHz, $CDCl_3$) δ 168.4, 166.6, 166.3, 157.2, 152.1, 148.9, 146.6, 144.1, 133.0, 131.0, 130.6, 130.4, 129.8, 129.3, 129.0, 128.4, 128.3, 128.0, 126.4, 140.3, 120.8, 95.5, 67.3, 59.1, 50.0, 39.6, 31.7, 31.0, 21.4, 17.5, 7.4. HRMS calcd for $C_{40}H_{38}N_4O_7S$: 719.2534 [M + H]$^+$; found, 719.2517 [M + H]$^+$.

Compound 9g. Yield 54%; mp 130−132 °C; t_R-HPLC, 3.78 min (96.2%). IR (KBr) ν cm^{-1}: 3343, 3262, 2966, 2930, 1750, 1660, 1615, 1558, 1459, 1278, 1248, 1148, 1088, 814, 687; ^{1}H NMR ($CDCl_3$, 400 MHz) δ 8.38 (s, 1H, C7−H), 8.22 (d, 1H, J = 8.4 Hz, C12−H), 7.92 (d, 1H, J = 8.0 Hz, C9−H), 7.82 (t, 1H, C11−H), 7.75 (d, 1H, J = 8.0 Hz, C11−H), 7.65 (t, 1H, C10−H), 7.30 (d, 2H, J = 8.0 Hz, Ts-H), 7.25 (s, 1H, C14−H), 7.02 (d, 2H, J = 8.8 Hz, -PhOCH$_3$), 6.77 (d, 2H, J = 8.8 Hz, -PhOCH$_3$), 5.32 (Abq, 2H, J = 17.6 Hz, C17−H), 5.22 (s, 2H, C5−H), 4.24−4.29 (m, 3H, C23,C30−H), 3.74 (s, 3H, -PhOCH$_3$), 2.42 (s, 3H, Ts-CH$_3$), 2.33 (m, 3H, C18−H, L-leucine-CH$_2$CH(CH$_3$)$_2$), 1.20 (m, 1H, L-leucine-CH$_2$CH(CH$_3$)$_2$), 0.92 (t, 3H, C19−H), 0.85 (m, 6H, L-leucine−CH(CH$_3$)$_2$); ^{13}C NMR (100 MHz, $CDCl_3$) δ: 170.6, 167.0, 159.3, 157.0, 152.1, 148.8, 146.6, 145.1, 143.3, 131.1, 131.0, 129.8, 129.6, 129.0, 128.3, 128.1, 128.0, 126.4, 126.3, 123.9, 142.1, 140.2, 119.9, 114.8, 96.2, 67.1, 55.2, 50.0, 42.1, 40.8, 38.6, 31.7, 24.8, 22.6, 21.5, 7.5. HRMS calcd for $C_{42}H_{42}N_4O_8S$: 763.2796 [M + H]$^+$; found, 763.2776 [M + H]$^+$.

dx.doi.org/10.1021/jm5003588 | J. Med. Chem. 2014, 57, 6008−6018

Compound 9h. Yield 48%; mp 125−127 °C; t_R-HPLC, 3.82 min (97.0%). IR (KBr) ν cm^{-1}: 3391, 3238, 2955, 1754, 1664, 1603, 1542, 1498, 1402, 1279, 1235, 1143, 1086, 1040, 810, 693; ^1H NMR ($CDCl_3$, 400 MHz) δ 8.39 (s, 1H, C7−H), 8.29 (d, 1H, J = 8.4 Hz, C9−H), 7.93 (d, 1H, J = 8.0 Hz, C12−H), 7.83 (t, 1H, C11−H), 7.76 (d, 2H, J = 8.4 Hz, Ts-H), 7.66 (t, 1H, C10−H), 7.36 (s, 1H, C14−H), 7.25−7.20 (m, 3H, Ts-H, Ph-H), 7.14−7.12 (m, 4H, Ph-H), 5.48 (ABq, 2H, J = 17.2 Hz,C17−H), 5.26 (s, 2H, C5−H), 4.88 (m, 1H,C23−H), 4.03−4.36 (m, 2H, C30−H), 2.34 (s, 3H, Ts-CH_3), 2.11−2.21 (m, 2H, C18−H), 1.56−1.79 (m, 2H, L-leucine-CH_2CH-(CH_3)$_2$), 1.48 (m, 1H, L-leucine-CH(CH_3)$_2$), 0.93 (m, 3H, C19−H), 0.83−0.93 (m, 6H, L-leucine−CH(CH_3)$_2$); ^{13}C NMR (100 MHz, $CDCl_3$) δ 170.6, 166.9, 166.3, 157.3, 152.1, 148.8, 146.6, 145.1, 132.5, 131.0, 130.0, 129.8, 129.6, 129.4, 129.0, 128.3, 128.1, 128.0, 126.4, 140.3, 120.1,96.1, 67.2, 52.3, 50.0, 42.1, 40.8, 39.5, 31.7, 24.8, 22.8, 21.5, 7.5. HRMS calcd for $C_{41}H_{40}N_4O_7S$: 733.2690 $[M + H]^+$; found, 733.2670$[M + H]^+$.

Compound 9i. Yield 58%; mp 127−129 °C; t_R-HPLC, 4.95 min (95.2%). IR(KBr) ν cm^{-1}: 3339, 3259, 2932, 1752, 1666, 1617, 1514, 1459, 1402, 1279, 1250, 1140, 1085, 1038, 896, 753, 677, 553; ^1H NMR ($CDCl_3$, 400 MHz) δ 8.38 (s, 1H, C7−H), 8.19 (d, 1H, J = 8.4 Hz, C9−H), 7.94 (d, 1H, J = 8.4 Hz, C12−H), 7.81 (t, 1H, C11−H), 7.74 (d, 2H, J = 8.0 Hz, Ts-H), 7.68 (t, 1H, J = 8.0 Hz, C10−H), 7.40 (d, 2H, J = 8.4 Hz, -PhOCH_3), 7.36 (s, 1H, C14−H), 7.17 (d, 2H, J = 8.0 Hz, Ts-H), 7.03(d, 2H, J = 8.8 Hz, -PhOCH_3), 5.50 (ABq, 2H, J = 17.2 Hz,C17−H), 5.26 (s, 2H, C5−H), 4.66 (m, 1H, C23−H), 4.33 (s, 2H, C30−H), 3.73 (s, 3H, -PhOCH_3), 2.39 (s, 3H, Ts-CH_3), 2.11−2.21 (m, 2H, C18−H), 1.92−1.98 (m, 1H, L-isoleucine-CH(CH_3)-CH_2CH_3), 0.78−1.26 (m, 11H,C19−H, L-isoleucine-H); ^{13}C NMR (100 MHz, $CDCl_3$) δ 168.2, 166.6, 166.4, 159.6, 157.2, 152.1, 148.9, 146.7, 144.8, 131.7, 131.0, 129.7, 129.6, 129.0, 128.3, 128.2, 128.0, 126.4, 124.6, 142.4, 140.2, 120.8, 115.1, 95.5, 67.5, 58.3, 55.3, 50.1, 42.1, 38.9, 37.9, 31.8, 24.9, 21.5, 15.0, 11.3, 7.4. HRMS calcd for $C_{42}H_{42}N_4O_8S$: 763.2796 $[M + H]^+$; found, 763.2788 $[M + H]^+$.

Compound 9j. Yield 54%; mp 125−127 °C; t_R-HPLC, 3.72 min (96.2%). IR (KBr) ν cm^{-1}: 3339, 3258, 2966, 1751, 1666, 1619, 1539, 1454, 1401, 1280, 1258, 1142, 1085, 1051, 989, 693, 553; ^1H NMR ($CDCl_3$, 400 MHz) δ 8.38 (s, 1H, C7−H), 8.20 (d, 1H, J = 8.8 Hz, C12−H), 7.94 (d, 1H, J = 8.0 Hz, C9−H), 7.81 (t, 1H, C11−H), 7.75 (d, 2H, J = 8.0 Hz, Ts-H), 7.67 (t, 1H, C10−H), 7.50 (m, 4H,Ts, Ph-H), 7.37 (s, 1H, C14−H), 7.18 (d, 2H, J = 8.0 Hz, Ph-H), 7.00 (s, 1H, Ph-H), 5.51 (ABq, 2H, J = 17.6 Hz, C17−H), 5.26 (s, 2H, C5−H), 4.66 (m, 1H, C23−H), 4.40 (s, 2H, C30−H), 2.37 (s, 3H, Ts-CH_3), 1.90−2.23 (m, 3H, C18−H, L-isoleucine-CH(CH_3)CH_2CH_3), 1.14 (m, 2H, L-isoleucine−CH(CH_3)CH_2CH_3), 0.78−0.86 (m, 9H, C19−H, L-isoleucine−CH(CH_3)CH_2CH_3); ^{13}C NMR (100 MHz,$CDCl_3$) δ 168.2, 166.6, 166.0, 157.2, 152.2, 148.9, 146.7, 144.0, 133.0, 131.0, 130.6, 130.4, 129.8, 129.0,128.4, 128.3, 128.2, 128.1, 126.2, 142.2, 140.3, 120.9, 95.5, 67.4, 50.1, 42.2, 39.7, 37.4, 31.8, 24.9, 21.4, 15.0, 11.3, 7.4. HRMS calcd for $C_{41}H_{40}N_4O_7S$: 733.2690 $[M + H]^+$; found, 733.2669 $[M + H]^+$.

Compound 9k. Yield 52%; m.p.102−104 °C; t_R-HPLC, 5.36 min (96.4%). IR (KBr) ν cm^{-1}: 3385, 3262, 2929, 1750, 1663, 1611, 1544, 1451, 1280, 1246, 1144, 1048, 812, 757, 693, 552; ^1H NMR ($CDCl_3$, 400 MHz) δ 8.39 (s, 1H, C7−H), 8.22 (d, 1H, J = 8.4 Hz, C9−H), 7.95 (d, 1H, J = 8.0 Hz, C12−H), 7.82 (m, 3H, C11−H, Ts-H), 7.67 (t, 1H, C10−H), 7.36 (s, 1H, C14−H), 7.21 (d, 2H, J = 8.0 Hz, Ts-H), 7.17−7.15 (m, 3H, L-phenylalanine-Ph), 7.10 (d, 2H, J = 8.4 Hz, -PhOCH_3), 6.99−7.02 (m, 2H, L-phenylalanine-Ph), 6.89 (d, 2H, J = 8.8 Hz, -PhOCH_3), 5.50 (ABq, 2H, J = 17.2 Hz, C17−H), 5.26 (s, 2H, C5−H), 4.91 (m, 1H, C23−H), 4.23 (s, 2H, C30−H), 3.78 (s, 3H, -PhOCH_3), 3.12−3.06 (m, 2H, L-phenylalanine-CH_2), 2.39 (s, 3H, Ts-CH_3), 2.11−2.21 (m, 2H, C18−H), 0.81 (m, 3H, C19−H); ^{13}C NMR (100 MHz, $CDCl_3$) δ 169.0, 166.7, 166.4, 159.4, 157.2, 152.2, 148.9, 146.2, 144.3, 134.8, 131.5, 131.0, 129.8, 129.4, 129.1, 128.6, 128.4, 128.2, 128.1, 127.2, 126.4,124.0, 142.2, 140.3, 120.5, 114.9, 95.9, 67.2, 55.3, 54.9, 50.1, 38.7, 36.6, 32.0, 21.4, 7.4. HRMS calcd for $C_{45}H_{40}N_4O_8S$: 797.2640 $[M + H]^+$; found, 797.2661 $[M + H]^+$.

Compound 9l. Yield 35%; mp 123−125 °C; t_R-HPLC, 3.20 min (100%). IR (KBr) ν cm^{-1}: 3419, 3269, 2925, 1751, 1644, 1601, 1540, 1401, 1277, 1236, 1139, 1087, 1050, 814, 758, 699, 552; ^1H NMR ($CDCl_3$, 400 MHz) δ 8.45 (s, 1H, C7−H), 8.13 (d, 1H, J = 8.4 Hz, C9−H), 7.97 (d, 1H, J = 8.0 Hz, C12−H), 7.87 (t, 1H, C11−H), 7.71 (t, 1H, C10−H), 7.65 (d, 2H, J = 8.4 Hz, Ts-H), 7.36 (s, 1H, C14−H), 7.22 (d, 2H, J = 8.0 Hz, Ts-H), 7.17−7.20 (m, 5H, L-phenylalanine-Ph), 5.52 (ABq, 2H, J = 17.2 Hz, C17−H), 5.26 (s, 2H, C5−H), 4.91(m, 1H, C-23H), 4.11 (m, 2H, -CH_2OH), 3.14−3.23 (m, 2H, L-phenylalanine-CH_2), 2.39 (s, 3H, Ts-CH_3), 2.11−2.21 (m, 2H, C18−H), 0.91 (m, 3H, C19−H); ^{13}C NMR (100 MHz, $CDCl_3$) δ 167.7, 166.6, 166.5, 157.1, 152.1, 148.1, 145.8, 144.4, 135.1, 132.1, 131.3, 129.5, 129.4, 129.1, 129.0, 128.8, 128.5, 128.4, 128.3, 127.2, 126.4, 140.2, 121.0, 96.4, 67.2, 58.9, 56.1, 50.1, 37.5, 35.6, 32.0, 21.4, 7.5. HRMS calcd for $C_{39}H_{36}N_4O_8S$ 743.2146 $[M + Na]^+$; found, 743.2158 $[M + Na]^+$.

Cell Lines and Cytotoxicity Assay. The human tumor cell lines used in this work were A-549 (lung carcinoma), DU-145 (hormone-insensitive prostate cancer), KB (originally isolated from epidermoid carcinoma of the nasopharynx), KBvin (vincristine-resistant KB subline), and HCT116 (colorectal adenocarcinoma). These cell lines were obtained from the Lineberger Comprehensive Cancer Center (UNC-CH) or from ATCC (Manassas, VA), except KBvin, which was a generous gift from Professor Y.-C. Cheng (Yale University). All cell lines were maintained and assayed in RPMI-1640 medium containing 2 mM L-glutamine and 25 mM HEPES (HyClone), supplemented with 10% heat-inactivated fetal bovine serum (HyClone), 100 μg/mL streptomycin, 100 IU/mL penicillin, and 0.25 μg/mL amphotericin B (Cellgro) in a humidified atmosphere containing 5% CO_2 in air. Compound stock solutions were prepared at 10 mM in DMSO and diluted with culture medium with the final DMSO concentration ≤0.01% (v/v), a concentration without effect on cell growth. The 4−6 × 10^3 cells/well were cultured for 72 h with various concentrations of test compounds in 96-well plates at 37 °C. The antiproliferative activities of compounds were determined by a sulforhodamine B assay according to the procedures developed and validated at NCI[30] and are expressed as IC_{50} (μM) values, which reduced the cell number by 50% compared with that of the vehicle control after 72 h of continuous treatment. Each assay was performed in triplicate with duplicated samples.

Morphological Observation. Morphological changes of culture cells were observed under a phase contrast microscope and photographed with a digital camera (Nikon, Japan).

Apoptosis Assessment. Apoptosis was detected by an Annexin V-FITC/propidium iodide double staining kit (BD Biosciences). A-549 cells were treated with **9a** for 24 or 48 h. Cells were harvested by trypsinization and washed with ice-cold PBS. Cells were labeled with annexin V-FITC and propidium iodide for 15 min at room temperature in the dark. Labeled cells were analyzed by an FACSCalibur flow cytometer (Becton Dickinson).

Cell Cycle Analysis. A-549 cells were fixed with ice-cold 70% EtOH followed by propidium iodide staining. Samples were analyzed by a flow cytometer for cell cycle determination. Population of each cell cycle phase was calculated based on the ploidy (<2N as sub-G1; 2N as G1; between 2N and 4N as S; and 4N as G2/M) and evaluated statistically by Student's t-test ($P < 0.01$).

Western Blot Analysis. Cells were harvested in PBS containing proteinase inhibitors and phosphatase inhibitors, and sonicated. Whole cell lysates were separated by SDS−PAGE and transferred to Immobilon P membrane (EMD Millipore). The membrane was incubated with primary antibody followed by labeling with horseradish peroxidase (HRP)-conjugated secondary antibody (EMD Millipore). A chemilluminence substrate kit (EMD Millipore) was used for the detection of membrane-bound HRP and visualized by a luminsence image analyzer, LAS4000 (Fuji Photo Film Co., Japan).

Antibodies. Antibodies to caspase-3, caspase-8, caspase-9, PARP, phospho-ATM (Ser1981), ATM, phospho-ATR (Ser428), phospho-Chk1 (Ser345), phospho-Chk2 (Thr68), Chk2, phospho-H2AX (Ser139), and phospho-p53 (Ser15) were purchased from Cell Signaling Technology. Antibodies against ATM, ATR, Chk1, and PUMA were from Santa Cruz Biotechnology. Antibodies against Topo I, Topo IIα, Topo IIβ, p53, FADD, BAX, Bcl-xL, and Bcl-2 were from

BD Biosciences. Antibody to β-actin was purchased from EMD Millipore.

Topoisomerase I Activity Assay in a Cell-Free System. One unit of recombinant human topoisomerase I enzyme (TopoGEN) was preincubated for 20 min at 37 °C with vehicle, **9a**, **1**, **3**, or SN-38 in a final volume of 20 μL of reaction buffer (10 mM Tris-HCl, pH 7.9, 1 mM EDTA, 150 mM NaCl, 0.1% BSA, 0.1 mM spermidine, and 5% glycerol) was then incubated with 250 ng of supercoiled plasmid DNA for 20 min. The supercoiled, relaxed, or nicked DNA was separated by 1% agarose gel in 1× TAE (Tris-Acetate-EDTA) buffer. Ethidium bromide stained agarose gel was photographed using Gel Doc XR (Bio-Rad).

Topoisomerase I Activity Assay. The Topo I activity test was performed using an assay kit (TopoGEN) according to the manufacturer's instructions. Nuclear extracts from **9a**-treated A-549 cells were incubated with supercoiled DNA (for Topo I) or catenated kDNA (for Topo II) for 30 min at 37 °C. The reaction mixture was separated by 1% agarose gel in 1× TAE buffer. The gel was stained with ethidium bromide and photographed using Gel Doc XR (Bio-Rad).

Xenograft Model Antitumor Assay. Five- to six-week-old female *nu/nu* mice (National Laboratory Animal Center, Taiwan) were inoculated subcutaneously with 2×10^6 human colorectal adenocarcinoma HCT116 cells in the flank. When the grafted tumor volume reached the average volume of 200 mm^3, mice were randomly divided into four groups ($n = 8$). The treatment regimen is shown in Table 2. Vehicle control and compound **9a** at 5 or 10 mg/kg were administered i.v. once a day (QD) for 7 days and then i.p. once a day to the end. As an experimental control group, 100 mg/kg of compound **3** was administered i.v. once a week (QWK) to the end. The length (L) and width (W) of the graft was measured every 3 to 4 days to the end, and the tumor volume was calculated as $LW^2/2$. Results were evaluated statistically by Student's t-test. This study was approved by the Institutional Animal Care and Use Committee (IACUC) of the National Taiwan University (Taipei, Taiwan) and was performed according to the institutional guidelines.

Pathological Evaluation of in Vivo Toxicity. Sixty 8-week-old male BALB/c mice (National Laboratory Animal Center, Taipei, Taiwan) were used to evaluate single-dose toxicity. Mice were randomly divided into six groups ($n = 10$) and received a single i.p. injection of **9a** at 0 (vehicle), 30, 100, 200, or 300 mg/kg on day 0. One group was untreated as the normal control. Body weight was measured every 3 days for 15 days. At the end of experimental period, all animals were euthanized by CO_2, and tissues from the liver, lung, kidney, and spleen were weighed (data not shown). Tissues were fixed with 10% formalin and embedded in paraffin. Sections 3−5 μm in thickness were prepared for histopathological examination. Hematoxylin and eosin (H&E) stained paraffin sections were evaluated histopathologically according to the guideline described by Shackelford et al.,[36] and the symptomatic lesions were graded. The degree of lesions were graded from one to five depending on severity as follows: nothing significant, 1 = minimal (<1%), 2 = slight (1−25%), 3 = moderate (26−50%), 4 = moderately severe (51−75%), and 5 = severe/high (76−100%). Statistically significant results ($P < 0.05$) were shown. This study was approved by the Institutional Animal Care and Use Committee (IACUC) of China Medical University (Taichung, Taiwan) and was performed according to the institutional guidelines.

■ ASSOCIATED CONTENT

Supporting Information

HPLC results and conditions for **9a**−**9l**. This material is available free of charge via the Internet at http://pubs.acs.org.

■ AUTHOR INFORMATION

Corresponding Authors

*(Y.Q.L.) Phone: +86(0)931-8618795. Fax: +86(0)931-8915686. E-mail: yqliu@lzu.edu.cn.

*(K.H.L.) Phone: 919-962-0066. Fax: 919-966-3893. E-mail: khlee@email.unc.edu.

Notes

The authors declare no competing financial interest.

■ ACKNOWLEDGMENTS

This work was supported financially by the National Natural Science Foundation of China (30800720 and 31371975), the Post-Doctor Research Foundation (20090450142); and the Fundamental Research Funds for the Central Universities (lzujbky-2013-69). Support from U.S. NIH grant (CA177584) awarded to K.H.L. is also acknowledged. This study was also supported in part by the Taiwan Ministry of Health and Welfare Clinical Trial Center of Excellence (MOHW103-TDU-B-212-113002) and China Medical University Hospital Cancer Research Center of Excellence, Taiwan (MOHW103-TD-B-111-03).

■ ABBREVIATIONS USED

ATM, ataxia telangiectasia mutated; ATR, ataxia telangiectasia and Rad3-related; Chk, checkpoint kinase; CPT, camptothecin; DIPC, *N,N′*-diisopropyl carbodiimide; DMAP, 4-dimethylaminopyridine; FADD, Fas-associated protein with death domain; PUMA, p53 upregulated modulator of apoptosis; TFA, trifluoroacetic acid; Topo, topoisomerase

■ REFERENCES

(1) Wall, M. E.; Wani, M.; Cook, C. E.; Palmer, K. H.; McPhail, A. T.; Sim, G. A. Plant antitumor agents. I. The isolation and structure of camptothecin, a novel alkaloidal leukemia and tumor inhibitor from *Camptotheca acuminata*. *J. Am. Chem. Soc.* **1966**, *88*, 3888−3890.

(2) Wang, H. K.; Morris-Natschke, S. L.; Lee, K. H. Antitumor agents 170. Recent advances in the discovery and development of topoisomerase inhibitors as antitumor agents. *Med. Res. Rev.* **1997**, *17*, 367−425 and literature cited therein..

(3) Oberlies, N. H.; Kroll, D. J. Camptothecin and taxol: historic achievements in natural products research. *J. Nat. Prod.* **2004**, *67*, 129−135.

(4) Hsiang, Y. H.; Hertzberg, R.; Hecht, S. M.; Liu, L. F. Camptothecin induces protein-linked DNA breaks via mammalian DNA topoisomerase I. *J. Biol. Chem.* **1985**, *260*, 14873−14878.

(5) Pommier, Y.; Kohlhagen, G. K.; Kohn, K. W.; Leteurtre, F.; Wani, M. C.; Wall, M. E. Interaction of an alkylating camptothecin derivative with a DNA base at topoisomerase I-DNA cleavage sites. *Proc. Natl. Acad. Sci. U.S.A.* **1995**, *92*, 8861−8865.

(6) Liew, S. T.; Yang, L. X. Design, synthesis and development of novel camptothecin drugs. *Curr. Pharm. Des.* **2008**, *14*, 1078−1097.

(7) Li, Q. Y.; Zu, Y. G.; Shi, R. Z.; Yao, L. P. Review camptothecin: current perspectives. *Curr. Med. Chem.* **2006**, *13*, 2021−2039.

(8) Rahier, N. J.; Thomas, C. J.; Hecht, S. M. Camptothecin and Its Analogs. In *Anticancer Agents from Natural Products*; Cragg, G. M., Kingston, D. G. I., Newman, D. J., Eds.; CRC Press: New York, 2012; pp 5−21, and literature cited therein.

(9) Adams, D. J. The impact of tumor physiology on camptothecin-based drug development. *Curr. Med. Chem.: Anti-Cancer Agents* **2005**, *5*, 1−13.

(10) Tobin, P. J.; Rivory, L. P. Camptothecins and key lessons in drug design. *Drug Des. Rev.* **2004**, *1*, 341−346.

(11) Hatefi, A.; Amsden, B. Camptothecin delivery methods. *Pharm. Res.* **2002**, *19*, 1389−1399.

(12) Onishi, H.; Machida, Y. Macromolecular and nanotechnological modification of camptothecin and its analogs to improve the efficacy. *Curr. Drug Discovery Technol.* **2005**, *2*, 169−183.

(13) Sirikantaramas, S.; Asano, T.; Sudo, H.; Yamazaki, M.; Saito, K. Camptothecin: therapeutic potential and biotechnology. *Curr. Pharm. Biotechnol.* **2007**, *8*, 196−202.

(14) Fassberg, J.; Stella, V. J. A kinetic and mechanistic study of the hydrolysis of camptothecin and some analogues. *J. Pharm. Sci.* **1992**, *81*, 676−684.
(15) Zhao, H.; Lee, C.; Sai, P.; Choe, Y. H.; Boro, M.; Pendri, A.; Guan, S.; Greenwald, R. B. 20-*O*-Acylcamptothecin derivatives: evidence for lactone stabilization. *J. Org. Chem.* **2000**, *65*, 4601−4606.
(16) Liu, Y. Q.; Tian, X.; Yang, L.; Zhan, Z. C. First synthesis of novel spin-labeled derivatives of camptothecin as potential antineoplastic agents. *Eur. J. Med. Chem.* **2008**, *43*, 2610−2614.
(17) Yang, L.; Zhao, C. Y.; Liu, Y. Q. Synthesis and biological evaluation of novel conjugates of camptothecin and 5-flurouracil as cytotoxic agents. *J. Braz. Chem. Soc.* **2011**, *22*, 308−318.
(18) Yang, L. X.; Pan, X.; Wang, H. J. Novel camptothecin derivatives. Part 1: oxyalkanoic acid esters of camptothecin and their in vitro and in vivo antitumor activity. *Bioorg. Med. Chem. Lett.* **2002**, *12*, 1241−1244.
(19) Cao, Z.; Harris, N.; Kozielski, A.; Vardeman, D.; Stehlin, J. S.; Giovanella, B. Alkyl esters of camptothecin and 9-nitrocamptothecin: synthesis, in vitro pharmacokinetics, toxicity, and antitumor activity. *J. Med. Chem.* **1998**, *41*, 31−37.
(20) De Groot, F. M. H.; Busscher, G. F.; Aben, R. W. M.; Scheeren, H. W. Novel 20-carbonate linked prodrugs of camptothecin and 9-aminocamptothecin designed for activation by tumour-associated plasmin. *Bioorg. Med. Chem. Lett.* **2002**, *12*, 2371−2376.
(21) Lerchen, H. G.; Baumgarten, J.; von dem Bruch, K.; Lehmann, T. E.; Sperzel, M.; Kempka, G.; Fiebig, H. H. Design and optimization of 20-*O*-linked camptothecin glycoconjugates as anticancer agents. *J. Med. Chem.* **2001**, *44*, 4186−4195.
(22) Greenhill, J. V.; Lue, P. Amidines and guanidines in medicinal chemistry. *Prog. Med. Chem.* **1993**, *30*, 203−326.
(23) Rauws, T. R. M.; Maes, B. U. W. Transition metal-catalyzed *N*-arylations of amidines and guanidines. *Chem. Soc. Rev.* **2012**, *41*, 2463−2497.
(24) Sondhi, S. M.; Dinodia, M.; Jain, S.; Kumar, A. Synthesis of biologically active *N*-methyl derivatives of amidines and cyclized five-membered products of amidines with oxalyl chloride. *Eur. J. Med. Chem.* **2008**, *43*, 2824−2830.
(25) Rahmathullah, S. M.; Hall, J. E.; Bender, B. C.; McCurdy, D. R.; Tidwell, R. R.; Boykin, D. W. Prodrugs for amidines: synthesis and anti-pneumocystis carinii activity of carbamates of 2,5-bis(4-amidinophenyl)furan. *J. Med. Chem.* **1999**, *42*, 3994−4000.
(26) Casini, A.; Scozzafava, A.; Mastrolorenzo, A.; Supuran, C. T. Sulfonamides and sulfonylated derivatives as anticancer agents. *Curr. Cancer Drug Targets* **2002**, *2*, 55−75.
(27) Nishino, R.; Ikeda, K.; Hayakawa, T.; Takahashi, T.; Suzuki, T.; Sato, M. Syntheses of 2-deoxy-2,3-didehydro-*N*-acetylneuraminic acid analogues modified by *N*-sulfonylamidino groups at the C-4 position and biological evaluation as inhibitors of human parainfluenza virus type 1. *Bioorg. Med. Chem.* **2011**, *19*, 2418−2427.
(28) Takasuna, K.; Kasai, Y.; Kitano, Y.; Mori, K.; Kobayashi, R.; Hagiwara, T.; Kakihata, K.; Hirohashi, M.; Nomura, M.; Nagai, E. Protective effects of kampo medicine and baicalin against intestinal toxicity of a new anticancer camptothecin derivative, irinotecan hydrochloride (CPT-11), in rats. *Jpn. J. Cancer Res.* **1995**, *86*, 978−984.
(29) Bae, I.; Han, H.; Chang, S. Highly efficient one-pot synthesis of *N*-sulfonylamidines by Cu-catalyzed three-component coupling of sulfonyl azide, alkyne, and amine. *J. Am. Chem. Soc.* **2005**, *127*, 2038−2039.
(30) Skehan, P.; Storeng, R.; Scudiero, D.; Monks, A.; McMahon, J.; Vistica, D.; Warren, J. T.; Bokesch, H.; Kenney, S.; Boyd, M. R. New colorimetric cytotoxicity assay for anticancer-drug screening. *J. Natl. Cancer Inst.* **1990**, *82*, 1107−1112.
(31) Li, T. K.; Liu, L. F. Tumor cell death induced by topoisomerase-targeting drugs. *Annu. Rev. Pharmacol. Toxicol.* **2001**, *41*, 53−77.
(32) Desai, S. D.; Zhang, H.; Rodriguez-Bauman, A.; Yang, J. M.; Wu, X.; Gounder, M. K.; Rubin, E. H.; Liu, L. F. Transcription-dependent degradation of topoisomerase I-DNA covalent complexes. *Mol. Cell. Biol.* **2003**, *23*, 2341−2350.
(33) Takemura, H.; Rao, V. A.; Sordet, O.; Furuta, T.; Miao, Z. H.; Meng, L.; Zhang, H.; Pommier, Y. Defective Mre11-dependent activation of Chk2 by ataxia telangiectasia mutated in colorectal carcinoma cells in response to replication-dependent DNA double strand breaks. *J. Biol. Chem.* **2006**, *281*, 30814−30823.
(34) Kastan, M. B.; Bartek, J. Cell-cycle checkpoints and cancer. *Nature* **2004**, *432*, 316−323.
(35) Kunimoto, T.; Nitta, K.; Tanaka, T.; Uehara, N.; Baba, H.; Takeuchi, M.; Yokokura, T.; Sawada, S.; Miyasaka, T.; Mutai, M. Antitumor activity of 7-ethyl-10-[4-(1-piperidino)-1-piperidino]-carbonyloxy-camptothecin, a novel water-soluble derivative of camptothecin, against murine tumors. *Cancer Res.* **1987**, *47*, 5944−5947.
(36) Shackelford, C.; Long, G.; Wolf, J.; Okerberg, C.; Herbert, R. Qualitative and quantitative analysis of nonneoplastic lesions in toxicology studies. *Toxicol. Pathol.* **2002**, *30*, 93−96.